RESEARCH ARTICLE

ES Cell-Derived Glial Precursors Contribute to Remyelination in Acutely Demyelinated Spinal Cord Lesions

Alberto Perez-Bouza; Tamara Glaser; Oliver Brüstle

Institute of Reconstructive Neurobiology, University of Bonn LIFE & BRAIN Center and Hertie Foundation, Bonn, Germany.
Corresponding author:
Oliver Brüstle, MD, Institute of Reconstructive Neurobiology, University of Bonn LIFE & BRAIN Center, Sigmund-Freud-Strasse 25, D-53105 Bonn, Germany
(E-mail: *brustle@uni-bonn.de*)

Pluripotent embryonic stem (ES) cells have emerged as a powerful tool for disease modeling and neural regeneration. Transplantation studies in rodents indicate that ES cell-derived glial precursors (ESGPs) efficiently restore myelin in dysmyelinating mutants and chemically induced foci of myelin loss. Here we explore the myelination potential of ESGPs in an antibody/complement-induced demyelination model. Microinjection of an antibody to myelin oligodendrocyte glycoprotein (MOG) and complement was employed to generate circumscribed areas of demyelination in the adult rat spinal cord. ESGPs transplanted into 2-day-old lesions were found to survive and differentiate into both oligodendrocytes and astrocytes. The engrafted cells remained largely confined to the lesion site and showed no evidence of tumor formation up until 4 weeks after transplantation. Within areas of pronounced microglial activation and macrophage extravasation, engrafted ES cell-derived oligodendrocytes contacted and enwrapped host axons and alongside endogenous glia, contributed to the formation of new myelin sheaths. These findings demonstrate that ESGPs transplanted into acutely demyelinated lesions can contribute to myelin repair.

Brain Pathology 2005;15:208-216.

INTRODUCTION

In human inflammatory demyelinating diseases such as multiple sclerosis (MS), spontaneous myelin repair by endogenous oligodendroglia occurs but is limited in its extent (7, 31, 32, 43). Transplantation of glial cells has been proposed as an alternative and complementary therapeutic strategy for the treatment of myelin disorders (10, 13). A key problem associated with this approach is the limited access to appropriate donor tissue. The advent of ES cell technology has provided new prospects for generating tissue-specific donor cells in virtually unlimited numbers in vitro. In addition to their self renewal capacity, ES cells are easily amenable to genetic modification and, due to their pluripotency, can differentiate into all somatic tissues and cell types (11, 26).

Several studies have focused on the generation of ES cell-derived oligodendrocytes (3, 5, 24, 28, 45, 46). In previous work, we have devised a protocol for the differentiation of murine ES cells into highly purified bipotential glial precursors and exploited them for myelin repair in the myelin-deficient rat, an animal model of Pelizaeus-Merzbacher disease. The transplanted cells efficiently myelinated host axons in the brain and spinal cord, without evidence for tumor formation or other deleterious side effects (5). In another set of experiments, ES cells induced to differentiate with retinoic acid were shown to form myelin upon transplantation into the spinal cord of *shiverer* mice and foci of lysolecithin-induced chemical demyelination (24). Very recently, human ES cell-derived oligodendrocytes were shown to be capable of myelinating host axons in the *shiverer* mouse brain, indicating that ES cell-based transplantation strategies for myelin repair can be translated to human cells (28).

While dysmyelinating mutants such as the *shiverer* mouse and the myelin-deficient rat are appropriate model systems for exploring the myelination capacity of glial transplants, they lack the pronounced reactive and inflammatory changes observed in demyelinating disorders such as MS. In that regard, experimental autoimmune encephalomyelitis (EAE) has become the most widely used animal model of MS (40). The paradigm has, however, 2 major limitations for the evaluation of transplant studies. First, as in MS, the disease shows pronounced interindividual variations. Although some immunization paradigms have been shown to result in preferential demyelination of distinct regions such as the optic nerve or the spinal cord (36), the exact localization of the lesions within these compartments remains largely unpredictable, precluding a precise targeting of cell transplants to the affected areas. Second, the transplanted cells themselves are at risk to succumb to the autoimmune response.

Antibody/complement-induced demyelination has been employed as an alternative model to study remyelination in the CNS. Typically, co-injection of an antibody to an oligodendrocyte/myelin epitope such as galactocerebroside and complement is used to induce circumscribed foci of demyelination (44). Along these lines, we established an anti-MOG/complement-based rat model, which results in pronounced localized demyelination, microglial activation, perivascular inflammatory changes, reactive astrogliosis and robust axon preservation. This model system was used to address the basic question whether ES cell-derived glial precursors can differentiate into oligodendrocytes and myelinate axons in an environment exhibiting morphological features also observed in acute stages of inflammatory myelin disorders (1). Our data show that ESGPs engrafted into foci of antibody/complement-induced demyelination survive, differentiate and contribute to myelin repair.

MATERIAL AND METHODS

ES cell differentiation. Mouse ES cell lines J1 or CJ7 (22, 37) were expanded

on gamma-irradiated mouse embryonic fibroblasts in Dulbecco's modified Eagle's medium (DMEM; Life Technologies/Invitrogen, Karlsruhe, Germany) containing 20% fetal bovine serum (FBS; Biochrom AG Seromed, Berlin, Germany), nonessential amino acids (Life Technologies), 8 mg/L adenosine, 8.5 mg/L guanosine, 7.3 mg/L cytidine, 7.3 mg/L uridine, 2.4 mg/L thymidine, 0.1 mM 2-mercaptoethanol, 26 mM HEPES (all from Sigma, Taufkirchen, Germany) and 10^3 U/ml human recombinant leukemia inhibitory factor (LIF, Chemicon, Hofheim, Germany). ES cell differentiation was performed as previously described (5, 41). Briefly, ES cells were passaged onto gelatin-coated dishes, trypsinized and transferred to non-adherent bacterial dishes allowing for embryoid body (EB) formation in the absence of LIF. Four-day-old EBs were plated onto tissue culture dishes and further propagated in DMEM/F12 (Life Technologies) containing 5 µg/ml insulin, 50 µg/ml human APO transferrin (both from Intergene, Purchase, NY), 30 nM sodium selenite (Sigma), 2.5 µg/ml fibronectin and penicillin/streptomycin (both from Life Technologies) according to Okabe et al (29). After 5 days, cells were trypsinized, triturated to a single cell suspension, replated on laminin-coated dishes (1 µg/ml; Life Technologies) and further propagated in DMEM/F12 supplemented with 25 µg/ml insulin, 50 µg/ml transferrin, 30 nM sodium selenite, 20 nM progesterone (Sigma), 100 nM putrescine (Sigma), 10 ng/ml fibroblast growth factor 2 (FGF-2; R&D Systems, Wiesbaden-Nordenstadt, Germany) and penicillin/streptomycine (Sigma). To enrich for glial precursors, cells were dissociated and further propagated in the same medium supplemented with 10 ng/ml FGF-2 and 20ng/ml epidermal growth factor (EGF). Cells were then passaged at a 1:3 to 1:5 ratio and again grown to subconfluency in the presence of 10 ng/ml FGF-2 and 10 ng/ml patelet-derived growth factor (PDGF-AA). In vitro differentiation was induced by growth factor withdrawal. Cells were cultured in a 37°C incubator under a 5% CO_2 atmosphere.

Retroviral infection of ESGPs. pREV-PLAP retrovirus was produced from stably transfected GP+E-86 helper cells (12, 25). Two days before transduction, cells were plated at a density of 3×10^6 cells per 10-cm dish. After 24 hours, the medium was switched to serum-free DMEM/F12. 24 hours later, the medium was harvested, filtered through 0.45-µm-pore filters and immediately used for transduction.

ES cell-derived glial precursors (growing in the presence of FGF-2 and EGF) were plated at a density of 3×10^6 cells per 10-cm dish. After 24 hours, the cells were incubated for 2 hours with polybrene (4 µg/ml) and subsequently exposed to the virus supernatant. Fresh medium was added after another 3 hours. A complete medium change was performed after 20 hours.

Experimental inflammatory demyelination. All animal experiments were performed according to institutional guidelines. Twelve- to 13-week-old female Sprague-Dawley rats were anesthetized with an intraperitoneal injection of xylazine (Rompun®, 10 mg/kg) and ketamine (Ketanest®, 80 mg/kg). After clamping of the 13th thoracic and the first lumbar vertebrae with a Cunningham rat spinal cord adaptor (Stoelting), a laminectomy was performed. Using a glass micropipette with a bore size of 20 to 30 µm connected to a stereotaxic device, 4 µl of a cocktail containing MOG antibody (clone 8-18-C5, 5 mg/ml, a gift from Chris Linington, Institute of Medical Sciences, University of Aberdeen), and guinea pig complement (Harlan Sera-Lab, United Kingdom) in 0.1 M sterile PBS (Gibco) at a ratio of 1:1:3 (MOG/complement/PBS) were slowly injected (1 µl/min) into the dorsal white matter tracts 600-700 µm below the dura. The pipette was left in place for 5 minutes to allow spread of the fluid and prevent back-flow into the injection trajectory. To exclude unspecific demyelination by complement or anti-MOG itself, control animals (n = 5) received complement/PBS or anti-MOG/PBS injections. All rats were treated with daily intraperitoneal injections of cyclosporin (10 mg/kg; Sandimmun, Novartis).

Preparation of the donor cells for transplantation. ESGPs growing in the presence of FGF-2 and PDGF were rinsed 3× in Hanks-EDTA, trypsinized and harvested as a single cell suspension. After neutralization with soybean trypsin inhibitor (Sigma), cells were centrifuged at 300 g at 4°C and washed in Hanks' buffered saline solution-EDTA (HBSS, Invitrogen) containing 0.1% DNAse (Sigma). They were then concentrated in Hank's buffered salt solution to 75.000 cells/µl and kept on ice until transplantation. Trypan blue exclusion showed that donor cells prepared in this manner exhibit viability rates ranging from 80% to 90%.

Cell transplantation. Two days after induction of demyelination, animals were reoperated, and 1 µl of a cell suspension containing 75.000 ESGPs was injected into the demyelinated area using the architecture of the local vasculature as landmark. A glass micropipette with 50 to 75 µm fire-polished orifice was used for transplantation. Cells were injected over 5 minutes at 600 µm below the dura. All animals received daily injections of cyclosporin, starting 2 days before surgery (see above).

Tissue processing. Seven, 14, 21 or 28 days after transplantation, rats were deeply anesthetized and fixed by intracardial perfusion with 4% paraformaldehyde (PFA) in 0.1 M PBS. Spinal cords were dissected and post-fixed overnight in the same fixative. Specimens from animals which had received PLAP-overexpressing cells were cut in 70-µm coronal sections on a vibratome (Leica). Every second section was processed either for immunofluorescence or electron microscopy. The remaining tissues were cryoprotected in 15% sucrose in 0.1 M PBS for at least three days. Twenty-µm thick coronal or horizontal cryostat sections were serially cut in a freezing Microtome (Microm), collected on SuperFrost®-plus slides (Meinzl-Glaeser, Germany) and stored at -80°C. The horizontal sections were found particularly useful to visualize and trace the dorsal white matter tracts and the demyelinated axons across several centimeters within the same optical plane.

In situ hybridization. For donor cell identification, sections were hybridized with a probe to mouse satellite DNA as described (6). The probe recognizes highly repetitive tandem sequences located in the centromeric heterochromatin (17). Briefly, sections were digested with 1 µg/ml pronase (Sigma) in 2× SSC, 0.5mM EDTA at 37°C for 20 minutes, rinsed in 2× SSC, dehydrated in ascending alcohol concentrations and air-dried. DNA denaturation was

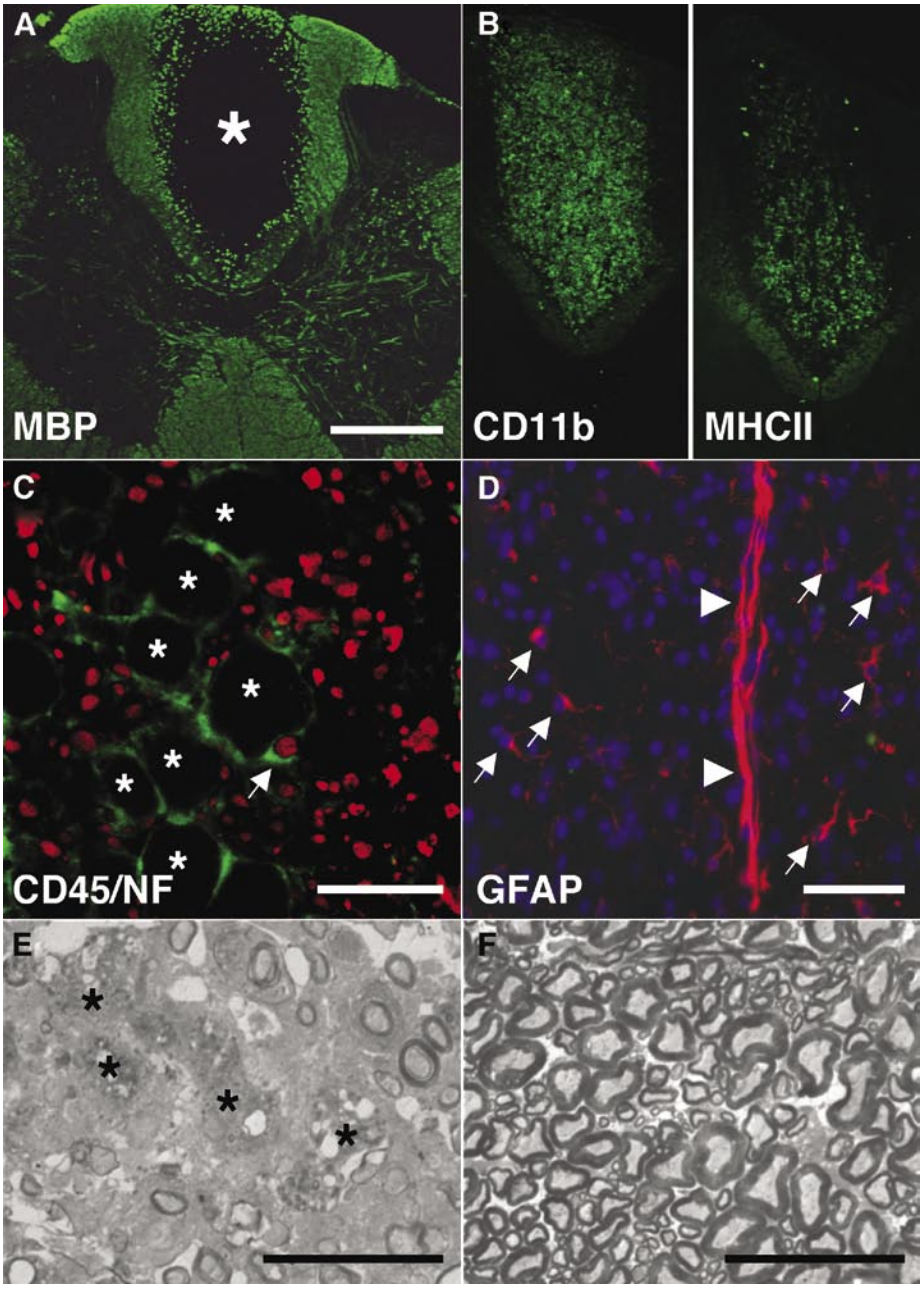

Figure 1. Inflammatory demyelination observed 7 days after injection of MOG antibody and guinea pig complement into the dorsal funiculus of the adult rat spinal cord. **A.** The demyelinating lesions in the dorsal funiculus are characterized by a sharply demarcated lack of MBP immunoreactivity (asterisk). **B.** In adjacent sections, immunofluorescence analyses with antibodies to CD11b and MHCII reveal a pronounced microglial/macrophage activation. The reactive changes closely correspond to the MBP-deficient areas shown in (**A**). **C.** Within the demyelinated areas, neurofilament-positive axons (red) are surrounded by large round CD45-positive inflammatory cells (asterisks, green). The arrow depicts a CD45-positive inflammatory cell with a cytoplasmic expansion around a neurofilament-positive axon (confocal microscopy; 1 µm optical slice). **D.** Demyelinated areas lacking MBP immunoreactivity contain numerous GFAP-positive astrocytes with short cytoplasmic processes (red, arrows). Prominent GFAP-positive astrocytic processes are detectable around blood vessels (red, arrowheads). **E.** A semithin section stained with Toluidine blue shows pronounced myelin loss. Asterisks depict debris-filled macrophages. **F.** Normal myelination in a control animal 7 days after PBS-injection. Scale bars: **A-B**: 500 µm, **C**: 20 µm, **D**: 50 µm, **E, F**: 25 µm.

performed by treatment with 70% deionized formamide/2× SSC (pH 7,0) at 90°C for 12 minutes. Sections were dehydrated again in ascending alcohol concentrations at -20°C, dried on a 37°C heating plate and hybridized overnight at 37°C in 70% formamide, 2× SSC, 250 µg/ml salmon sperm DNA. The next day, sections were washed in 50% formamide in 2× SSC at 37°C, followed by another wash in 0.5× SSC at RT. Hybridized probe was detected with rhodamine- or peroxidase-conjugated antibodies to digoxigenin.

Immunohistochemistry. Immunohistochemical analyses were performed using primary antibodies to myelin basic protein (MBP; Chemicon, 1:500), placental alkaline phosphatase (PLAP; Abcam, 1:500), oligodendrocyte myelin glycoprotein (OMG; Serotec, 1:500), 2′, 3′-cyclic nucleotide 3′-phosphodiesterase (CNPase; Sigma, 1:200), glial fibrillary acidic protein (GFAP; Dako, 1:1000), 200 kD neurofilament (Sigma, 1:500), β-III-tubulin (TUJ1; Sigma, 1:1000), the microglial/macrophage marker CD11b (OX-42; Serotec, 1:50), MHCII (OX6; Serotec, 1:50) and CD45/LCA (leukocyte common antigen, Serotec, 1:200). With exception of anti-MBP and anti-OMG stainings, specimens were permeabilized with 0.1% Triton X-100 in 0.1 M PBS. For MBP and OMG immunohistochemistry, sections were treated for 10 minutes with 100% ethanol, and no detergents were used during the staining procedure. Primary antibodies were incubated overnight at room temperature in 0.1 M PBS with 5% NGS. No detergents or alcohol treatment were used for pre-embedding anti-PLAP immunohistochemistry (see below). Biotinylated, peroxidase-, FITC-, Cy3- or rhodamine-conjugated secondary antibodies (Dako and Jackson Laboratories, all diluted at 1:200) were incubated at room temperature for 2 hours in 0.1 M PBS with 5% NGS. For permanent antigen visualization, 3,3′-di-amino-benzidine (DAB; Dako) was used. When combined with fluorescence DNA in situ hybridization, immunofluorescence was performed using a tyramide amplification system (NEN/Perkin Elmer) to account for antigen destruction and signal reduction during the hybridization procedure. Following incubation with peroxidase-conjugated secondary antibodies, the sections were treated with tyramide/FITC or tyramide/biotin. Biotinylated tyramide was detected at the end of the procedure with either avidin/Texas-red or avidin/Cy-5 (Vector Laboratories, 1:200). 4′,6-Diamidino-2-phenylindole (DAPI, Sigma) was used for nuclear counterstaining. Sections were coverslipped in Vectashield® (Vector Laboratories) and sealed with nail polish.

Electron microscopy. Selected coronal sections subjected to pre-embedding DAB immunohistochemistry were post-fixed in 2% glutaraldehyde and 2% PFA in 0.1 M PBS, osmicated in 2% osmium-tetraoxide, dehydrated in ascending alcohol concentrations, plastic-embedded and serially cut on an ultramicrotome (Leica-Ultracut-R). Semithin sections were counterstained with 1% toluidine blue for conventional histological analysis. Ultrathin sections were slightly counterstained with uranyl acetate and lead citrate and analyzed on a Zeiss 900 electron microscope at 50 kV accelerating voltage.

Light microscopy, quantification and statistical analysis. Sections were analyzed on a Zeiss Axiophot-2 microscope with a Sony 3CCD-video camera connected to a PC equipped with a Zeiss KS-300 image analysis system. Confocal images were collected at a Zeiss LSM-510 using 3-channel immunofluorescence recording stacks of ≤1 µm optical sections. Quantification of the demyelinated lesions was performed by measuring the areas lacking MBP immunoreactivity in every 50th 20-µm thick coronal section and multiplying the values by the distance between sections. For statistical analysis the Mann-Whitney-U test was used.

RESULTS

Reactive inflammatory changes, astrogliosis and axonal preservation in anti-MOG/complement-induced lesions. The injection of 4 µl of anti-MOG/complement suspension into the dorsal funiculus of the spinal cord resulted in well-delineated, spindle-shaped areas of demyelination, which reached their maximal expansion 7 days after surgery. The lesions showed a lack of MBP and OMG immunoreactivity and were densely infiltrated by inflammatory cells displaying a rounded morphology and expression of the surface antigens CD45 (LCA), CD11b and MHCII (Figure 1A-C). Neurofilament-positive axons traversing these MBP-negative areas were tightly surrounded by CD45/LCA-positive inflammatory cells (Figure 1C). Seven days after lesioning, numerous GFAP-positive astrocytes with short cytoplasmic processes were found within the lesions (Figure 1D, arrows). GFAP immunolabeling was particularly pronounced around the blood vessels (Figure 1D, arrowheads), which may in part be due to facilitated access of the antibody to the perivascular spaces. After 23 days, hypertrophic astrocytes and a dense network of GFAP-positive processes were detectable both at the edge and within the core of the lesions (not shown). The lesions were associated with slight edema, and subtle tissue shrinkage and glial scarring were noted at the pial surface. Yet, the gross anatomy of the spinal cord was not altered. Microscopical analysis of semithin sections confirmed the pronounced loss of myelin and and infiltration by macrophages containing myelin debris (Figure 1E). Axons were seen to be surrounded by myelinophages but axonal clubbing was a rare event, suggesting a high degree of axonal preservation (not shown). Volumetric quantification of the lesions revealed that the combined injection of anti-MOG antibody and complement resulted in demyelinating lesions reaching a maximal volume 3.26 ± 0.86 mm^3 by day 7 after surgery. Starting from the second week after injection, macrophages containing myelin debris progressively disappeared from the lesions. Treatment with complement/PBS or anti-MOG/PBS only gave rise to circumscribed lesions around the injection site (Figure 2A). With increasing survival time, the volumes of the regions displaying a lack of MBP-immunoreactivity were seen to diminish from 3.26 ± 0.86 mm^3 at day 7 to 1.61 ± 0.12 mm^3 and 0.72 ± 0.29 mm^3 at day 16 and 23 after surgery, respectively (Figure 2B). Although we cannot exclude that subtle tissue resorption may have contributed to the reduction of the MBP-deficient areas, these data indicate that anti-MOG/complement-induced lesions exhibit a high degree of axonal integrity and spontaneous remyelination, arguing for a preservation of endogenous glial precursors.

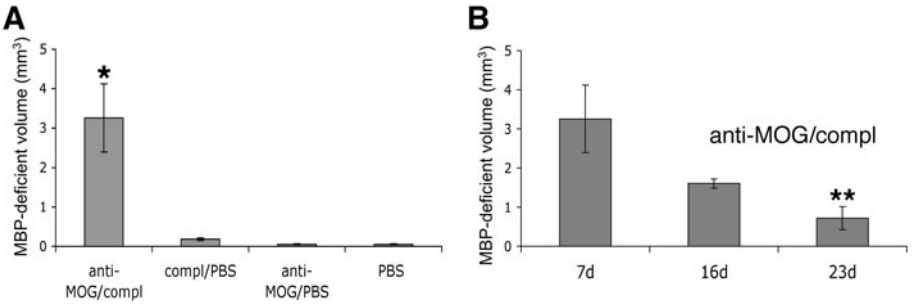

Figure 2. Specificity and time course of anti-MOG/complement-induced demyelination. **A.** Seven days after injection of anti-MOG and complement, the MBP-deficient regions encompass 3.26 ± 0.86 mm^3. In contrast, injections of complement/PBS, anti-MOG/PBS or PBS alone do not result in significant demyelination (*p<0,02). **B.** Between day 7 and day 23 after anti-MOG/complement injection, the MBP-deficient regions decrease significantly, suggesting endogenous remyelination. **p<0,01 (Mann-Whitney-U test). All values in A-B are represented as mean ±SEM.

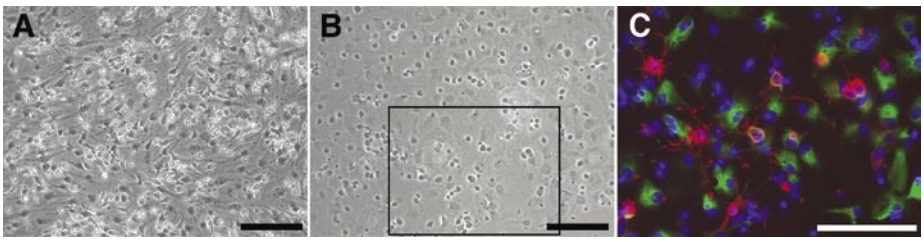

Figure 3. In vitro differentiation of ES cell-derived glial precursors (ESGPs). **A**. ESGPs proliferating in the presence of FGF2 and PDGF display an elongated bipolar morphology. The growth factor-mediated selection procedure has left numerous dead cells. Cells from this stage were used for transplantation. **B-C.** Four days after growth factor withdrawal, ESGPs have differentiated into both astrocytes and oligodendrocytes. Double immunofluorescence (C, higher magnification of area delinated in B) depicts 04-positive oligodendrocytes (red) and flat GFAP-positive astrocytes (green; nuclear counterstain: DAPI). Scale bars in **A-C**: 125 µm.

In vitro differentiation of wild-type and retrovirally transduced ESGPs. For donor cell preparation, ES cells were first differentiated into multipotent neural precursors. These pan-neural precursors were then shifted into a glial precursor fate by sequential propagation in FGF2/EGFand FGF2/PDGF (Figure 3A). This protocol has been shown to yield a highly purified population of ESGPs which readily differentiate into

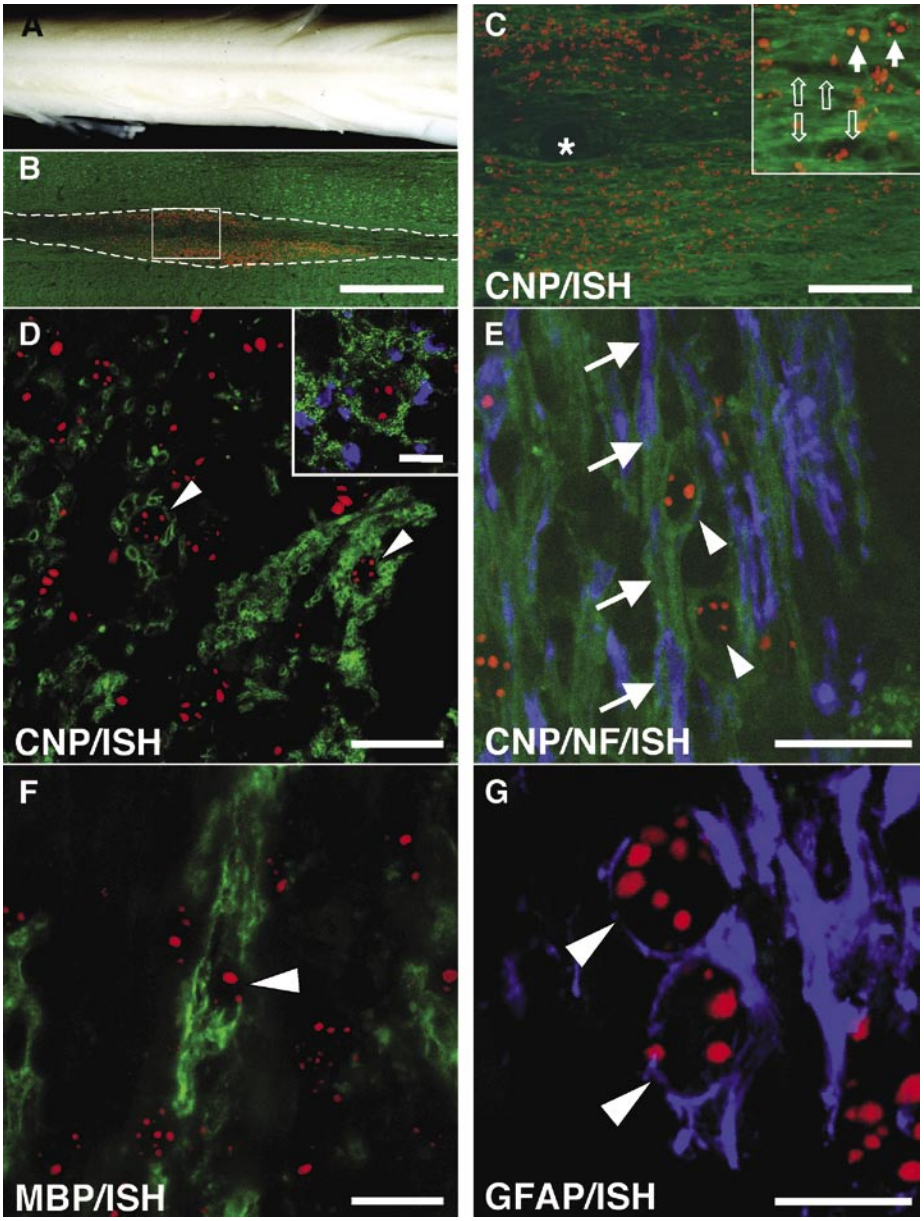

Figure 4. In vivo differentiation of ESGPs 2 weeks after transplantation. **A.** Macroscopic view of a transplanted spinal cord prior to histological processing. No tumor formation, gross mechanical damage or infection was noted in any of the transplant recipients. **B-C.** Horizontal sections at the level of the dorsal funiculus, hybridized with a mouse-specific DNA probe (red nuclear signal). **C** represents a higher magnification of the boxed region in **B**. Following injection, the donor cells remained mostly confined to the lesion sites (dashed line in **B**) and located preferentially to regions containing numerous CNP-positive cell processes (green immunofluorescence). Perivascular regions containing abundant inflammatory cells were typically devoid of donor cells and CNP immunoreactivity (asterisk in **C**). The inset in (**C**) illustrates the close association of CNP-positive cells derived from donor (hybridized mouse satellite DNA, filled arrows) and host (non-hybridized nuclei, open arrows). The presence of host nuclei was confirmed by phase contrast microscopy. Yet, in many cases, the relationship of the immunofluorescence signal to donor or host cell nuclei remained unresolved. **D.** In coronal sections, hybridized donor cells (arrowheads) frequently showed perinuclear CNP-positive circular extensions, which, upon triple labeling, were found to enwrap neurofilament-positive host axons (blue, inset). **E.** Longitudinal section depicting neurofilament-positive host axons (blue) which are enwrapped by CNP-positive processes (green) originating from hybridized donor cells (red nuclear signal). Arrows depict putative internodes generated by two CNP-positive donor cells (arrowheads). **F.** Hybridized donor cell (arrowhead) emanating putative MBP-positive internodes. **G.** Incorporated donor cells with perinuclear GFAP immunoreactivity indicating astrocytic differentiation. **D-G.** represent stacks of two to three 1-µm confocal slices. Scale bars: **B**: 1 mm; **C**: 250 µm, **D, F** and **G**: 20 µm; **E** and inset in **D**: 10 µm.

O4-positive oligodendrocytes and GFAP-positive astrocytes, (5). Similar to these previous studies, growth factor withdrawal for 4 days typically yielded 20% to 25% O4-positive oligodendrocytes with multipolar phenotypes and 30% to 35% GFAP-positive astrocytes displaying a flat morphology (Figure 3B-C).

Engrafted ESGPs survive and generate oligodendrocytes. Two days after anti-MOG/complement-injection, the lesions were engrafted with single cell suspensions of FGF-2/PDGF-treated ESGPs. Transplant recipients were sacrificed between day 7 and 28 after grafting. Macroscopic examination did not reveal any disruption of the gross anatomy or tumor formation in any of the recipient spinal cords at any survival time (Figure 4A). DNA in situ hybridization with a mouse-specific probe showed that the grafted cells had distributed bilaterally along the demyelinated foci. The donor cells remained largely confined to the lesion site with little spread across the anteroposterior and dorsoventral axes (Figure 4B). They appeared seamlessly integrated with the host tissue without signs of glial capsulation or cyst formation (Figure 4B-C). Confocal microscopy of hybridized cells provided evidence for the expression of CNP (Figure 4D-E) and MBP (Figure 4F) in the engrafted cells. In addition to oligodendrocytes, grafted ESGPs generated GFAP-positive astrocytes (Figure 4G). GFAP immunofluorescence also revealed reactive host astrocytes with thickened cell processes at the lesion/transplantation site (not shown). While these data are indicative of oligodendroglial and astrocytic differentiation of the donor cells, the resolution of our multilabeling system did not permit attribution of each hybridized nucleus to a distinct immunochemical phenotype (see inset, Figure 4C), thus precluding a quantification of ESGP-derived oligodendrocytes and astrocytes.

Engrafted ES cell-derived oligodendrocytes ensheath host axons. Fluorescence in situ hybridization in combination with double immunofluorescence analysis was used to study the relationship between donor cells and host axons in detail. High resolution confocal microscopy revealed that CNP-positive donor cells had formed processes emanating ring-like structures

around neurofilament-positive host axons (Figure 4D-E). Ensheathment of host axons by donor oligodendrocytes was also observed in transplants containing PLAP-expressing ESGPs (Figure 5). These experiments revealed seamlessly integrated clusters of PLAP-positive cells enwrapping a large number of beta-III-tubulin-positive host axons (Figure 5A-B). Ring-like PLAP-positive structures were CNP-positive, confirming oligodendroglial differentiation of the donor cells (Figure 5C). In addition, CNP-positive, PLAP-negative circular structures were detected within the lesions, suggesting axonal ensheathment by endogenous glia (Figure 5C, arrowheads). PLAP-negative and PLAP-positive ring structures were found in intimate association, without detectable interface. This observation suggests a close interaction of donor and host cells during remyelination.

ES cell-based myelin formation. Semithin sections containing PLAP-positive cells revealed bundles of thinly myelinated host axons surrounded by complex immunoreactive cells with oligodendroglial morphologies (Figure 5D). Focally, axons were also found to be myelinated by clusters of PLAP-negative endogenous Schwann cells (Figure 5E) and endogenous oligodendrocytes (not shown). In addition, intermingled PLAP-positive donor cells with no clear axonal contact were detected. These cells displayed short cytoplasmic processes compatible with an astrocytic phenotype (Figure 5E, arrow).

In ultrathin sections, the DAB precipitate indicating PLAP immunoreactivity was found to accumulate at the cell membrane as previously described (18) (Figure 6A-B). Donor-derived oligodendrocytes exhibited typical ultrastructural features such as clumped, electron-dense chromatin and a cytoplasmic matrix rich in organelles. Thinly myelinated host axons were seen enwrapped by oligodendroglial processes (Figure 6A) or in close association to them (Figure 6B). Compacted myelin sheaths around host axons revealed DAB precipitate at the outermost membrane, indicating donor cell-derived myelin formation (Figure 6B, inset).

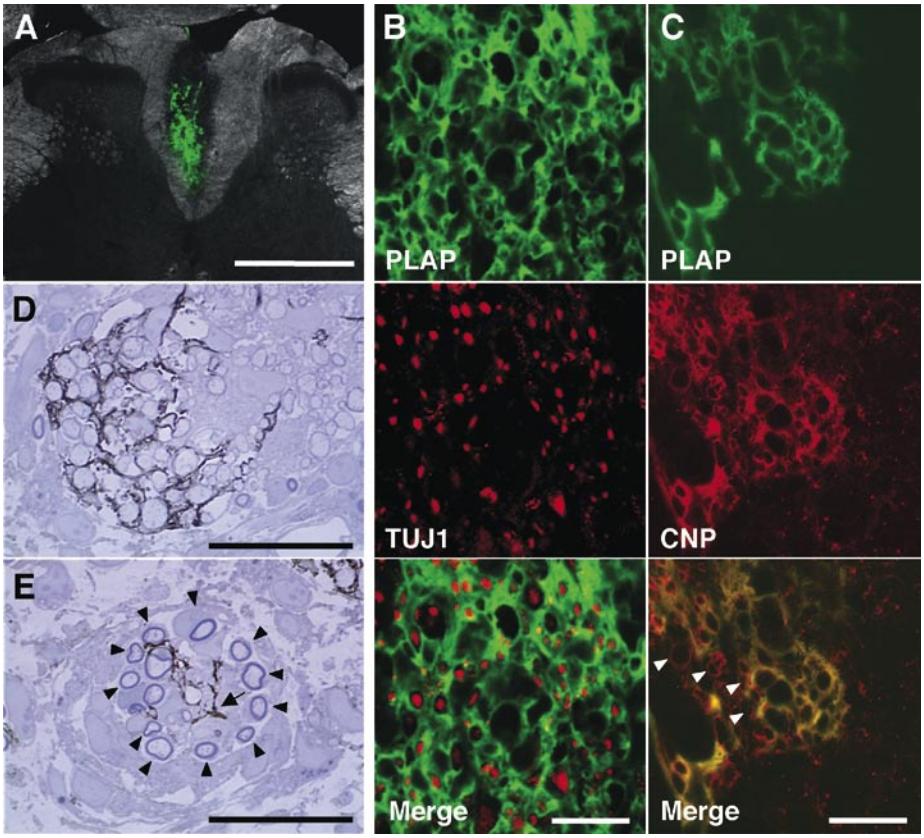

Figure 5. Oligodendroglial differentiation of retrovirally labeled ESGPs 3 weeks after implantation. **A.** Overview of a coronal section containing a cluster of retrovirally PLAP-labeled cells (green) within the previously demyelinated dorsal funiculus. The donor cells are restricted to the demyelinated area. **B-C.** Confocal microphotographs of sections adjacent to (**A**), labeled with antibodies to PLAP (**B-C**, green), beta-III-tubulin (TUJ1, **B**, red) and CNP (**C**, red). PLAP-positive donor cells frequently generated honeycomb-like structures around beta-III-tubulin-positive host axons (**B**). Double labeling revealed a close spatial association of PLAP-positive and PLAP-negative (**C**, arrowheads) periaxonal CNP-positive structures, suggesting cooperation of donor and host cells in axon remyelination. **D-E.** Detection of PLAP-positive transplanted cells in semithin sections. Thinly myelinated host axons are enwrapped by immunolabeled donor cell processes (**D**). **E.** In some regions, ramified donor cells with astrocyte-like DAB-labeled processes (arrow) were found in close association with Schwann cells (arrowheads) myelinating small axon bundles. Schwann cells were consistently PLAP-negative, arguing for a host origin. Scale bars: **A**: 1 mm; **B-C**: 20 µm; **D-E**: 25 µm.

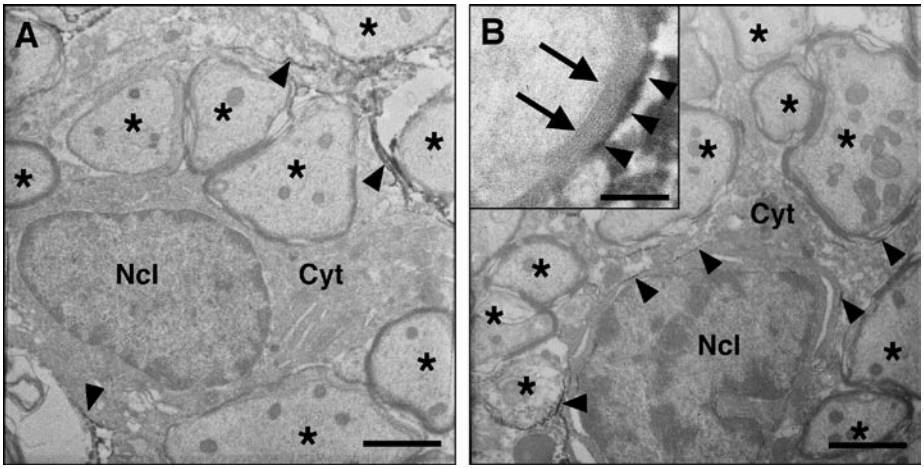

Figure 6. Electron micrographs of myelinating ES cell-derived oligodendrocytes 3 weeks after transplantation into areas of anti-MOG/complement-induced demyelination. **A-B.** The engrafted cells exhibit an electron-dense, clumped chromatin and a cytoplasmic matrix rich in organelles. Donor cells are identified by dark membrane-associated DAB precipitate indicating PLAP immunoreactivity (arrowheads). Asterisks indicate adjacent host axons at different stages of myelination. The inset in (**B**) shows a high magnification of compacted donor-derived myelin (arrows) with PLAP immunoprecipitate attached to the outermost lamella (arrowheads). Ncl, nucleus; Cyt, cytoplasma. Scale bars in **A** and **B**: 2 µm, inset in **B**: 0.5 µm.

DISCUSSION

The results of this study demonstrate that ES cell-derived glial precursors (ESGPs)

implanted into foci of demyelination, microglial activation, perivascular inflammatory changes and reactive astrogliosis can differentiate into mature oligodendrocytes which myelinate host axons. Following transplantation, the engrafted cells remain largely confined to the site of demyelination, where they differentiate into both astrocytes and oligodendrocytes. The ES cell-derived oligodendrocytes establish contact with the demyelinated host axons and, alongside endogenous oligodendrocytes and Schwann cells, generate new myelin sheaths. In a previous study we have shown that highly purified, non-tumorigenic ES-GPs can be used to restore myelin in the brain and spinal cord of myelin-deficient rats (5). The current study extends these data to demyelinated lesions displaying many histopathological features of inflammatory myelin diseases.

In the past, a variety of animal models have been used to explore the myelination potential of glial grafts. Primary oligodendroglial precursors and cell lines derived from CNS tissue have been shown to generate myelin after neonatal transplantation into myelin-deficient mutants such as the *shiverer* mouse, the myelin-deficient rat or the shaking pup (10). In adult recipients, injection of ethidium bromide (EB) in combination with X-irradiation has frequently been used to create demyelinated areas suitable for assaying the myelination capacity of transplanted glial cells (4, 14, 15). EAE models, which most closely mimic the pathological changes observed in MS, have rarely been used for studying transplant-based remyelination. Following transplantation of the oligodendrocyte precursor cell line CG4 or primary neural precursors, a more widespread distribution of the donor cells was observed in hosts with EAE compared to healthy controls (2, 38). The results of a recent study by Pluchino et al. indicate that adult neurospheres, injected either systemically or into the cerebral ventricles, can form myelin and induce behavioral recovery in a mouse EAE model. It remains, however, unclear to what extent the functional restoration observed is due to donor-derived myelin formation rather than transplant-based bystander effects promoting endogenous myelin repair (30).

Considering the complexity of systemic autoimmune models, we selected a localized antibody/complement-mediated demyelination paradigm to study donor cell differentiation and myelin formation in an environment mimicking many morphological features of inflammatory myelin diseases (1). Local injection of antibodies to myelin and oligodendrocyte antigens along with complement has been shown to yield circumscribed demyelinated areas with good preservation of axons and endogenous progenitors capable of myelin repair (44). Similarly, the anti-MOG/complement injection used here reproducibly gave rise to demyelinating lesions with a high degree of axonal preservation, reactive astrogliosis and pronounced infiltration with CD45-positive leukocytes, microglia and macrophages, ie, features observed in acute stages of inflammatory myelin disorders (1). The target antigen used in our study—MOG—was long considered a marker of differentiated oligodendrocytes (8, 33-35). Recently, this glycoprotein has also been detected in NG2- and PDGFR-alpha-positive oligodendrocyte progenitors of the adult rat spinal cord (23). Although we cannot exclude collateral damage to endogenous oligodendrocyte progenitors in our system, the pronounced rate of spontaneous remyelination indicates that anti-MOG/complement-induced demyelination leaves the majority of the host oligodendrocyte progenitors intact. While our experimental model exhibits many of the morphological features found in acutely demyelinated lesions, it cannot reproduce the complex and still largely unknown immunological mechanisms and interactions between hematopoietic and neural cells involved in the pathogenesis of MS. On the other hand, it is this lack of an underlying systemic immune response which makes the process of demyelination predictable and thus more accessible to the study of donor cell incorporation and differentiation.

The influence of activated microglia, macrophages and reactive astrocytes on the process of demyelination and subsequent remyelination is still a matter of debate (21). Microglia and macrophages have been shown to positively influence myelin formation in vitro (9, 16). There is evidence that depletion of macrophages and a lack of insulin-like growth factor-1 (IGF-1) production by microglia, macrophages and astrocytes inhibit remyelination (20, 27). On the other hand, macrophages and activated microglial cells are known to produce a variety of toxic mediators, including TNF-α, reactive oxygen and nitrogen species and excitotoxins (21). Experiments in myelin mutants have shown that activated microglia inhibits survival and function of transplanted oligodendrocyte progenitors (47). While the results of our study demonstrate that ES cell-derived glial precursors survive and differentiate into myelinating oligodendrocytes in a reactive and inflammatory environment, it remains to be investigated whether pharmaceutical modulation of the inflammatory response could be exploited to enhance donor- and host-mediated myelination in this model. This issue is closely related to the question of whether the reactive and inflammatory environment and the exposure to demyelinated axons influence the in vivo differentiation of the donor cells. A detailed quantification of ES cell-derived oligodendrocytes, myelin and astrocytes would be required to comprehensively address this issue. In the model employed, we found such an approach severely hampered by the limited ability to allocate CNP-positive internodes and astrocyte processes to distinct donor or host cell bodies (Figures 4C, 5C). While the quantification of MBP-immunonegative areas served as a useful indicator of tissue damage and myelin loss following antibody/complement injection, the heterogeneous distribution of transplanted oligodendrocytes throughout the lesions precluded a quantification of myelination by such area measurements. Further studies involving donor cells expressing GFP fused to myelin proteins could provide a more detailed quantitative evaluation of donor cell-mediated remyelination

A key prerequisite for the development of ES cell-based therapies is the generation of highly purified, non-tumorigenic donor cells. The step-wise differentiation paradigm used here has proven an efficient tool for the enrichment of glial precursors and the elimination of undifferentiated, tumorigenic cells. Consequently, no evidence of teratoma formation or non-neural donor-derived tissues was noted in this and our previous study (5). Yet, it is important to stress that the design of our current study does not permit a thorough assessment of tumorigenicity and that long-term studies in rodents and more long-lived recipient species are required to comprehensively as-

sess safety and post-repair functional performance of myelinating ES cell transplants.

One of the major problems associated with the development of transplant-based myelin repair strategies is the necessity to deliver donor cells to multiple sites throughout the CNS. While our study aims at providing first data on the differentiation and myelination capacity of ESGPs implanted into a strongly inflammatory lesion, localized stereotaxic implants will most likely not suffice to achieve widespread delivery of myelinating cells to the brain and spinal cord. The results of a recent study in mice suggest that adult neural precursors injected intrathecally or intravenously can invade multiple EAE lesions throughout the CNS (30). It will be interesting and important to study whether this phenomenon can be translated to our donor cells and whether ESGPs administered via the blood or CSF show homing and myelin formation in EAE lesions. Long-term observations in EAE models will also have to address the susceptibility of transplanted oligodendrocytes to the systemic autoimmune response. Since axonal loss is increasingly recognized as limiting factor for functional recovery (19, 39), future strategies for transplant-based myelination might have to be complemented by donor cell-mediated release of neuroprotective factors. Finally, the development of cell-based myelination therapies will critically depend on the ability to translate rodent data into a human setting. Both fetal and adult human oligodendrocyte progenitors have been shown to myelinate the rodent CNS (42). Recently, human ES cell-derived oligodendrocytes were used for remyelinating transplants in *shiverer* mice (28). Future studies will have to address the question whether and to what extent human ES-derived oligodendrocytes can be exploited for myelin repair in inflammatory demyelination.

ACKNOWLEDGMENTS

This work was supported by the Deutsche Forschungsgemeinschaft (SFB 400), the Hertie Foundation, the Institute for Multiple Sclerosis Research (University Göttingen), the EU project QLG3-CT-2000-00911 and the Alexander von Humboldt-Foundation (research grant of A.P-B.). We gratefully acknowledge Chris Linington for providing the MOG antibody and his advice in the initial stages of the project. We thank Michaela Segschneider, Rachel Buschwald, Katja Klein and Karen Tolksdorf for excellent technical support and Tanja Schmandt for her help in editing the manuscript. The pREV-PLAP retrovirus was kindly provided by Jean-Luc Darlix and Isabelle Franceschini.

REFERENCES

1. Adams CW, Poston RN and Buk SJ (1989) Pathology, histochemistry and immunocytochemistry of lesions in acute multiple sclerosis. *J Neurol Sci* 92:291-306.

2. Ben-Hur T, Einstein O, Mizrachi-Kol R, Ben-Menachem O, Reinhartz E, Karussis D and Abramsky O (2003) Transplanted multipotential neural precursor cells migrate into the inflamed white matter in response to experimental autoimmune encephalomyelitis. *Glia* 41:73-80.

3. Billon N, Jolicoeur C, Ying QL, Smith A and Raff M (2002) Normal timing of oligodendrocyte development from genetically engineered, lineage-selectable mouse ES cells. *J Cell Sci* 115:3657-3665.

4. Blakemore WF, Crang AJ and Patterson RC (1987) Schwann cell remyelination of CNS axons following injection of cultures of CNS cells into areas of persistent demyelination. *Neurosci Lett* 77:20-24.

5. Brüstle O, Jones KN, Learish RD, Karram K, Choudhary K, Wiestler OD, Duncan ID and McKay RD (1999) Embryonic stem cell-derived glial precursors: a source of myelinating transplants. *Science* 285:754-756.

6. Brüstle O, Maskos U and McKay RD (1995) Host-guided migration allows targeted introduction of neurons into the embryonic brain. *Neuron* 15:1275-1285.

7. Chang A, Tourtellotte WW, Rudick R and Trapp BD (2002) Premyelinating oligodendrocytes in chronic lesions of multiple sclerosis. *N Engl J Med* 346:165-173.

8. Coffey JC and McDermott KW (1997) The regional distribution of myelin oligodendrocyte glycoprotein (MOG) in the developing rat CNS: an in vivo immunohistochemical study. *J Neurocytol* 26:149-161.

9. Diemel LT, Copelman CA and Cuzner ML (1998) Macrophages in CNS remyelination: friend or foe? *Neurochem Res* 23:341-347.

10. Duncan ID, Grever WE and Zhang SC (1997) Repair of myelin disease: strategies and progress in animal models. *Mol Med Today* 3:554-561.

11. Evans MJ and Kaufman MH (1981) Establishment in culture of pluripotential cells from mouse embryos. *Nature* 292:154-156.

12. Franceschini IA, Feigenbaum-Lacombe V, Casanova P, Lopez-Lastra M, Darlix JL and Dalcq MD (2001) Efficient gene transfer in mouse neural precursors with a bicistronic retroviral vector. *J Neurosci Res* 65:208-219.

13. Franklin RJ (2002) Remyelination of the demyelinated CNS: the case for and against transplantation of central, peripheral and olfactory glia. *Brain Res Bull* 57:827-832.

14. Franklin RJ, Gilson JM, Franceschini IA and Barnett SC (1996) Schwann cell-like myelination following transplantation of an olfactory bulb-ensheathing cell line into areas of demyelination in the adult CNS. *Glia* 17:217-224.

15. Groves AK, Barnett SC, Franklin RJ, Crang AJ, Mayer M, Blakemore WF and Noble M (1993) Repair of demyelinated lesions by transplantation of purified O-2A progenitor cells. *Nature* 362:453-455.

16. Hamilton SP and Rome LH (1994) Stimulation of in vitro myelin synthesis by microglia. *Glia* 11:326-335.

17. Hörz W and Altenburger W (1981) Nucleotide sequence of mouse satellite DNA. *Nucleic Acids Res* 9:683-696.

18. Jemmerson R, Klier FG and Fishman WH (1985) Clustered distribution of human placental alkaline phosphatase on the surface of both placental and cancer cells. Electron microscopic observations using gold-labeled antibodies. *J Histochem Cytochem* 33:1227-1234.

19. Kornek B, Storch MK, Weissert R, Wallstroem E, Stefferl A, Olsson T, Linington C, Schmidbauer M and Lassmann H (2000) Multiple sclerosis and chronic autoimmune encephalomyelitis: a comparative quantitative study of axonal injury in active, inactive, and remyelinated lesions. *Am J Pathol* 157:267-276.

20. Kotter MR, Setzu A, Sim FJ, Van Rooijen N and Franklin RJ (2001) Macrophage depletion impairs oligodendrocyte remyelination following lysolecithin-induced demyelination. *Glia* 35:204-212.

21. Lassmann H (2004) Experimental autoimmune encephalomyelitis. In: *Myelin Biology and Disorders* (R. A. Lazzarini, Griffin, J.W., Lassmann, H, Nave, K.A., Miller, R.H. and Trapp, B.D., ed), pp 1040-1071. San Diego, CA, USA: Elsevier.

22. Li E, Bestor TH and Jaenisch R (1992) Targeted mutation of the DNA methyltransferase gene results in embryonic lethality. *Cell* 69:915-926.

23. Li G, Crang AJ, Rundle JL and Blakemore WF (2002) Oligodendrocyte progenitor cells in the adult rat CNS express myelin oligodendrocyte glycoprotein (MOG). *Brain Pathol* 12:463-471.

24. Liu S, Qu Y, Stewart TJ, Howard MJ, Chakrabortty S, Holekamp TF and McDonald JW (2000) Embryonic stem cells differentiate into oligodendrocytes and myelinate in culture and after spinal cord transplantation. *Proc Natl Acad Sci U S A* 97:6126-131.

25. Lopez-Lastra M, Gabus C and Darlix JL (1997) Characterization of an internal ribosomal entry segment within the 5′ leader of avian reticuloendotheliosis virus type A RNA and development of novel MLV-REV-based retroviral vectors. *Hum Gene Ther* 8:1855-1865.

26. Martin GR (1981) Isolation of a pluripotent cell line from early mouse embryos cultured in medium conditioned by teratocarcinoma stem cells. *Proc Natl Acad Sci U S A* 78:7634-7638.

27. Mason JL, Suzuki K, Chaplin DD and Matsushima GK (2001) Interleukin-1beta promotes repair of the CNS. *J Neurosci* 21:7046-7052.

28. Nistor GI, Totoiu MO, Haque N, Carpenter MK and Keirstead HS (2005) Human embryonic stem cells differentiate into oligodendrocytes in high purity and myelinate after spinal cord transplantation. *Glia* 49:385-396.

29. Okabe S, Forsberg-Nilsson K, Spiro AC, Segal M and McKay RD (1996) Development of neuronal precursor cells and functional postmitotic neurons from embryonic stem cells in vitro. *Mech Dev* 59:89-102.

30. Pluchino S, Quattrini A, Brambilla E, Gritti A, Salani G, Dina G, Galli R, Del Carro U, Amadio S, Bergami A, Furlan R, Comi G, Vescovi AL and Martino G (2003) Injection of adult neurospheres induces recovery in a chronic model of multiple sclerosis. *Nature* 422:688-694.

31. Prineas JW, Barnard RO, Kwon EE, Sharer LR and Cho ES (1993) Multiple sclerosis: remyelination of nascent lesions. *Ann Neurol* 33:137-151.

32. Scolding N, Franklin R, Stevens S, Heldin CH, Compston A and Newcombe J (1998) Oligodendrocyte progenitors are present in the normal adult human CNS and in the lesions of multiple sclerosis. *Brain* 121 (Pt 12):2221-2228.

33. Scolding NJ, Frith S, Linington C, Morgan BP, Campbell AK and Compston DA (1989) Myelin-oligodendrocyte glycoprotein (MOG) is a surface marker of oligodendrocyte maturation. *J Neuroimmunol* 22:169-176.

34. Slavin AJ, Johns TG, Orian JM and Bernard CC (1997) Regulation of myelin oligodendrocyte glycoprotein in different species throughout development. *Dev Neurosci* 19:69-78.

35. Solly SK, Thomas JL, Monge M, Demerens C, Lubetzki C, Gardinier MV, Matthieu JM and Zalc B (1996) Myelin/oligodendrocyte glycoprotein (MOG) expression is associated with myelin deposition. *Glia* 18:39-48.

36. Storch MK, Stefferl A, Brehm U, Weissert R, Wallstrom E, Kerschensteiner M, Olsson T, Linington C and Lassmann H (1998) Autoimmunity to myelin oligodendrocyte glycoprotein in rats mimics the spectrum of multiple sclerosis pathology. *Brain Pathol* 8:681-694.

37. Swiatek PJ and Gridley T (1993) Perinatal lethality and defects in hindbrain development in mice homozygous for a targeted mutation of the zinc finger gene Krox20. Genes Dev 7:2071-2084.

38. Tourbah A, Linnington C, Bachelin C, Avellana-Adalid V, Wekerle H and Baron-Van Evercooren A (1997) Inflammation promotes survival and migration of the CG4 oligodendrocyte progenitors transplanted in the spinal cord of both inflammatory and demyelinated EAE rats. *J Neurosci Res* 50:853-861.

39. Trapp BD, Peterson J, Ransohoff RM, Rudick R, Mork S and Bo L (1998) Axonal transection in the lesions of multiple sclerosis. *N Engl J Med* 338:278-285.

40. Wekerle H, Kojima K, Lannes-Vieira J, Lassmann H and Linington C (1994) Animal models. *Ann Neurol* 36 Suppl: S47-53.

41. Wernig M, Tucker KL, Gornik V, Schneiders A, Buschwald R, Wiestler OD, Barde YA and Brustle O (2002) Tau EGFP embryonic stem cells: an efficient tool for neuronal lineage selection and transplantation. *J Neurosci Res* 69:918-924.

42. Windrem MS, Nunes MC, Rashbaum WK, Schwartz TH, Goodman RA, McKhann G, 2nd, Roy NS and Goldman SA (2004) Fetal and adult human oligodendrocyte progenitor cell isolates myelinate the congenitally dysmyelinated brain. *Nat Med* 10:93-97.

43. Wolswijk G (1998) Chronic stage multiple sclerosis lesions contain a relatively quiescent population of oligodendrocyte precursor cells. *J Neurosci* 18:601-609.

44. Woodruff RH and Franklin RJ (1999) Demyelination and remyelination of the caudal cerebellar peduncle of adult rats following stereotaxic injections of lysolecithin, ethidium bromide, and complement/anti-galactocerebroside: a comparative study. *Glia* 25:216-228.

45. Xian H and Gottlieb DI (2004) Dividing Olig2-expressing progenitor cells derived from ES cells. *Glia* 47:88-101.

46. Xian HQ, McNichols E, St Clair A and Gottlieb DI (2003) A subset of ES-cell-derived neural cells marked by gene targeting. *Stem Cells* 21:41-49.

47. Zhang SC, Goetz BD and Duncan ID (2003) Suppression of activated microglia promotes survival and function of transplanted oligodendroglial progenitors. *Glia* 41:191-198.